Vol. 23, No.4, PP. 28-37 P-ISSN: 2070-4003 E-ISSN: 2664-5548

Electrospun of PVP Nanofiber Doped with Au Nanoparticles for UV-Detector

Marwan S. Abdul Hamid^{1*} and Isam M. Ibrahim¹

¹Department of Physics, College of Science, University of Baghdad, Baghdad, Iraq *Corresponding author: marwan.abd2304@sc.uobaghdad.edu.iq

Abstract Article Info.

Pure polyvinylpyrrolidone (PVP) nanofibers were doped with different concentrations of gold nanoparticles (Au NPs) using the electrospinning technique. The characteristics of both nanofibers were investigated using Xray diffraction (XRD), field emission scanning electron microscope (FE-SEM), and UV-visible properties. The structure of PVP-Au was amorphous, as revealed by XRD. A DC voltage of 20 kV was applied to Au-PVP nanofiber beads on glass substrates and silicon wafers of n-Si type, oriented (111), at room temperature. The effect of doping on some physical properties (structural, optical, electrical, and sensitivity) of the polymer material was studied. The physical properties of the material composite film fibres were studied as the concentration of Au rises. The optical energy gap for three Au-PVP samples ranged between 3.60 and 3.70 eV. The responsivity for Au-PVP nanofibers was obtained for the UV detector, where the optimum detector sensitivity was at the wavelength of 360 nm. The sensitivity values obtained were 2.4, 17.5, and 24.45 for doping ratios 0.1:9.9, 0.5:9.5, and 1:9, respectively, with the values of the rise time ranging from 2.40 to 24.45s and fall time 10.2-22.3s for Au concentrations.

Keywords:

PVP, Nanofiber, Electrospinning, Flexible Defector, Thin Film.

Article history:

Received: Jun. 06,2024 Revised: Oct. 09, 2024 Accepted: Oct. 20, 2024 Published: Dec. 01, 2025

1. Introduction

Recently, researchers have shown a great interest in conductive polymers due to their unique properties such as low density, the ability to form intricate shapes, versatile electric properties, low manufacturing cost, and electronic, magnetic, and optical properties similar to those of metals. In addition, they maintain the environmental stability, flexibility, and processability of conventional polymers. One major benefit of conducting polymers is their easy production and the way their chemical structure changes to alter their physical characteristics, making them suitable for low-cost electrical devices. Povidone (PVP), also known as polyvinylpyrrolidone, with a chemical symbol (C₆H₉NO)n, is one of the most significant polymer types utilized in creating nanofibers. Vinylpyrrolidone is polymerized in an aqueous solution with hydrogen peroxide at the end of a multi-step production process to get PVP [1-7]. By adjusting the degree of polymerization, a broad range of molecular weights, from a few thousand to a few million, can be achieved. In contrast to many synthetic polymers, PVP is a white, hygroscopic powder soluble in a wide range of conventional solvents, including water, amides, alcohols, and amines [8]. The process of spinning in an electrostatic field produces microand nanometric nanofibers by elongating the droplets of spinning solutions in a strong, started electric field [9]. Many materials, such as metals, ceramics, natural and synthetic polymers, and composite systems, can be electrospun [10].

PVP nanofibers are highly adaptable materials with a wide range of applications. Their properties and ability to tailor their characteristics through composite formation make them indispensable in advancing technologies. PVP nanocomposite fibers can be highly effective in photodetectors, especially when combined with other nanomaterials, to enhance their light-absorbing and electrical properties. Incorporating metal

^{© 2025} The Author(s). Published by College of Science, University of Baghdad. This is an open-access article distributed under the terms of the Creative Commons Attribution 4.0 International License (https://creativecommons.org/licenses/by/4.0/).

nanoparticles (e.g., silver or gold) can improve light absorption due to Localized Surface Plasmon Resonance (LSPR), enhancing the overall sensitivity of the photodetector [11]. As electrospinning and electro-spraying share the same physical and electrical mechanics, they may be considered a natural progression of each other. The primary difference is that electro-spraying creates microscopic droplets, whereas electrospinning generates continuous strands [12].

In the last ten years, electrospinning has garnered a lot of interest because of its consistency in producing fibers in the sub-nanometre range and its adaptability in spinning a variety of polymeric fibre types. Nanofibers with a larger surface area and fewer holes than ordinary fibers derived from metals and metal composites, have several applications, including filtration, tissue scaffolding, infiltration, protective clothing, electro-optical, and electrical applications [13].

The aim of this study is to improve UV-detector sensitivity by doping PVP nanofibers with different concentrations of gold using electrospinning technique.

2. Experimental Work

The electrospun PVP solution was prepared by mixing 1 g of the polymer (90000 g/mol MW) with 11.4 ml alcohol and stirred at room temperature with a magnetic stirrer for 6 h. The gold nanoparticles (Au NPs) were prepared using the laser ablation technique where the used laser was Nd:YAG laser of 1064 nm with 200 pulses of 200 mJ power. The electrospinning solution was prepared by mixing Au with PVP solution at mixing ratios of 0.1:9.9, 0.5:9.5, and 1:9 and placed on a stirrer for 15 min at room temperature; these were designated as S1, S2, and S3, respectively. The colour of the Au-PVP composite was changed to a light pink meaning that Au nanoparticles were produced. Electrospinning installations come in two primary varieties: horizontal and vertical. For this experiment, the syringe pump was configured to operate in the horizontal setting, as indicated by Fig. 1. The three main components of the electric spinning system were: a syringe pump with a flow control range of 0.1 to 100 mL/h set at a flow rate of 0.5 mL/h, a DC high-voltage power source with an adjustable control range of (0-50 kV) set at 20 kV DC, and a conductive aluminium collector. The distance between the collector and the needle was 11 cm. The prepared Au-PVP solution was put into a syringe with its metal needle connected to the positive power supply to charge the polymer solution with a positive charge. The pure PVP solution was poured into the plastic syringe and forced into the pump. Because the aluminium collecting plate and syringe needle operate together to generate an electric field using high voltage, the electric field filled the plastic syringe and then released into the Taylor cone at a predetermined flow rate. The surface charge which was generated by the power source resulted in the production of a jet.

As the solvent evaporated on its way to the collecting plate, layer after layer of nanofibers was produced. The thickness of the sample was 300 nm. The influence on the structural morphology of the nanofibers was taken into consideration while determining the ideal electrospinning settings and operating conditions. The electrospun PVP solution was deposited on glass substrates to characterize the structural, surface morphology, and optical properties. It was also deposited on Si wafer for sensor preparation (Fig. 2).

The optical absorption spectra of the formed nanofibers as a function of wavelength (300–1100 nm) were obtained using UV–Vis spectrophotometer (Sp–800, Taiwan); this was done in Bagdad, Iraq. The X-ray diffraction (XRD) analyses were achieved in Iran using X-ray diffractometer (Shimadzu 6000, Japan). The surface morphology of the thin films was studied In Iran using field emission scanning electron microscope (FESEM) (MIRA3 model-TE-SCAN). The produced samples can be diagnosed by determining the effective aggregates and correlations between specific aggregates.

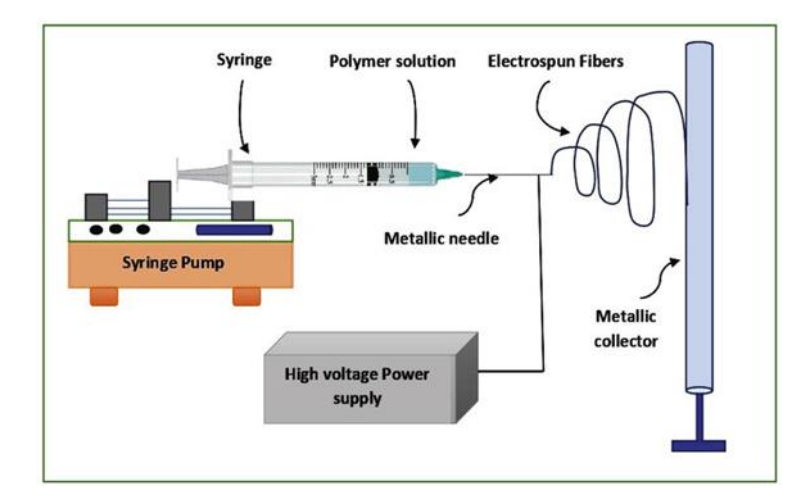


Figure 1: The electrospinning set-up.

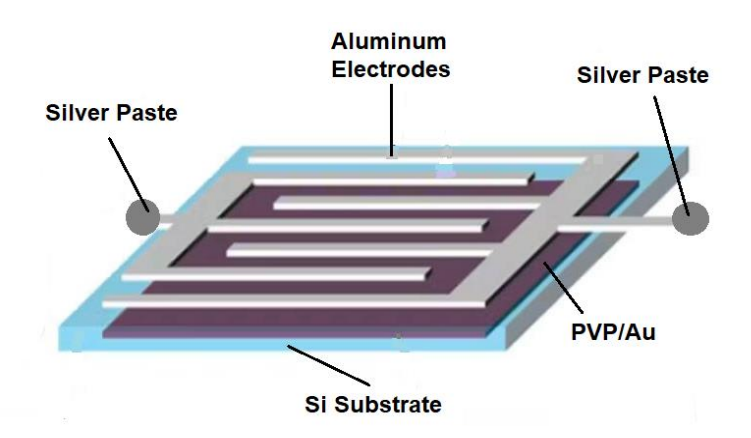


Figure 2: Cross section view of Pure PVP and PVP/Au doped.

3. Results and Discussion

3. 1. X-Ray Diffraction

The XRD patterns of the pure PVP, S1, S2, and S3 samples (where S1, S2 and S3 represents the mixing ratios Au with PVP of 0.1:9.9, 0.5:9.5, and 1:9 respectively) are shown in Fig. 3. The results showed that the material is amorphous and lacks directivity peaks, which is a feature shared by many other polymeric materials [14].

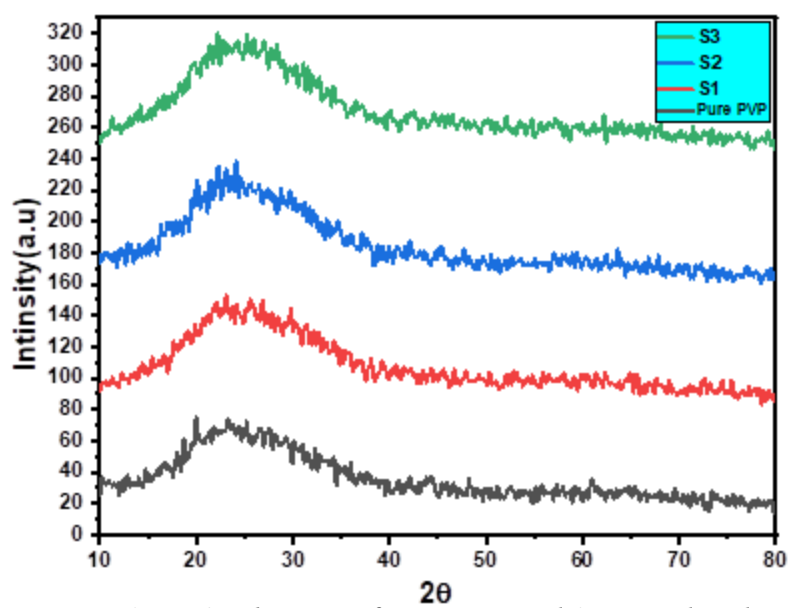


Figure 3: The XRD of Pure PVP and Au-PVP doped.

3. 2. Field Emission Scanning Electron Microscope

The examinations using a FESEM were done on the pure PVP and the three Au-PVP samples which were prepared using the three doping ratios of gold nanoparticles. The FESEM images obtained using a 1µm magnification (Fig. 4) showed the PVP nanofiber in a shape of mats. As seen in the images, the diameter of the nanofiber was approximately less than 100 nm according to the scale bar of the FESEM image; the gold nanoparticles have a size of 50 nm. The S3 sample (Au-PVP fibres with 1:9 doping ratio) is shown with mats and of several micros length and 130-540 nm width. The number of the mats increased with increasing the concentration of gold in the composite (as in S2 and S3). The formation of the mats has a correlation with the solution's viscoelasticity [15]. The viscoelastic force makes the jet smooth and continuous elongation into fibers possible throughout the electrospinning process [16]. The Au-PVP fibers were thinner than the PVP fibers, as shown by measuring the dimeters by ImageJ software. The fibers became thinner throughout the elongation phase as they approached the collector. The thinning process of the fiber reduces polymer chain entanglement, which causes the breakage of the fiber and produces beads in a low-viscosity solution [17]. A high viscoelastic characteristic might arise from increased inclusion of highly extensible compounds (polymers) into the precursor solution [15].

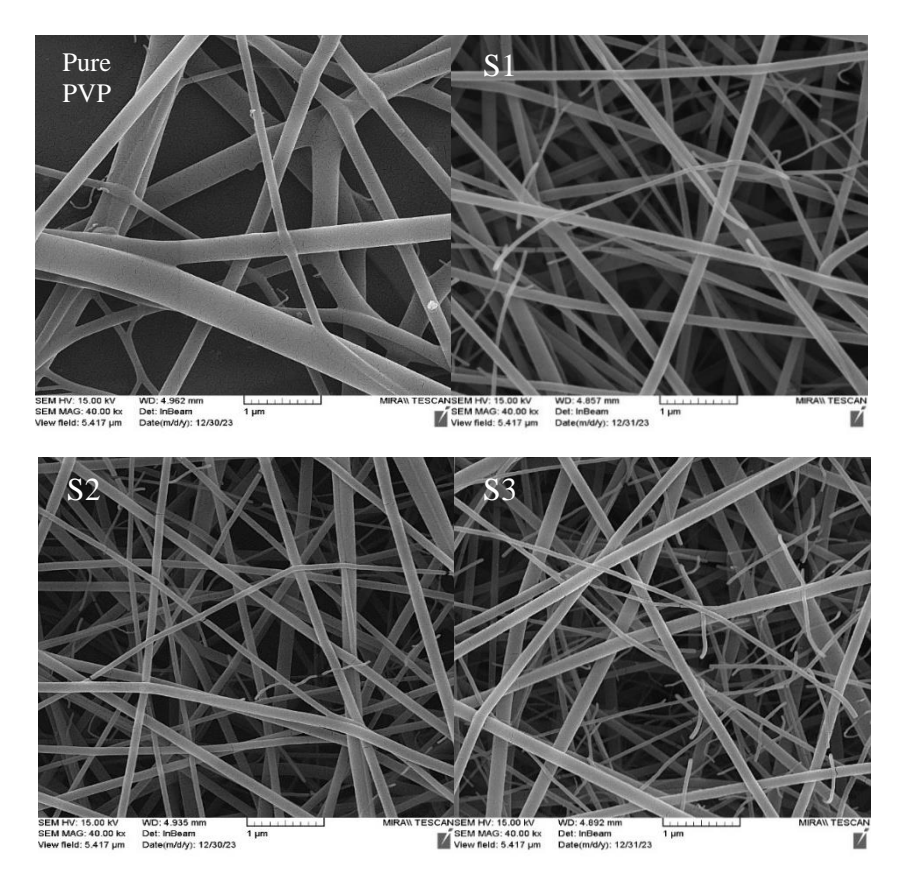


Figure 4: The SEM images of the pure PVP, S1, S2, and S3.

3. 3. Optical Characteristics

The optical characteristics of the PVP and PVP which were mixed with Au at different mixing ratios (S1, S2, and S3) were examined. The absorption coefficient α (v) was determined (using Equation 1) at the frequency linked to the high absorption region from the absorbance (A) and the film thickness (t) [18]

$$\alpha = 2.303 \,\mathrm{A/t} \tag{1}$$

The fundamental absorption edge is one of the most important features of the absorption spectra of crystalline and amorphous materials. The band gap of a material may be determined by calculating the fundamental absorption which is associated with the change from the valence to the conduction band. The optical energy band gap (E_g) calculation was made was made using Eq. (2) [19]

$$\alpha h \nu = \beta (h \nu - E_g)^r \tag{2}$$

where r is an index that characterizes the optical absorption process and has values of 1/2, 3/2, 2, or 3 depending on the kind of electronic transition that causes the absorption, and β is a constant depends on the probabilities of electron transitions [19, 20]. The absorption coefficient values for each electromagnetic radiation wavelength were determined using UV-Vis spectra. The linear portions of the $(\alpha h \nu)^2$ in the high absorption range were projected to zero absorption to determine the value of energy gap (Fig. 5). The energy gap of the pure PVP polymer nanofibers is 4.20 eV, which is in agreement with the previous study [6][20]. When Au nanoparticles were added to the PVP polymer solution with different doping ratios (S1, S2, and S3), the direct energy gap values of Au-PVP composite nanofibers dropped as the Au concentration increased, as shown in Table 1. PVP primarily absorbs light in the ultraviolet region due to electronic transitions associated with its pyrrolidone rings, specifically $n-\pi^*$ and $\pi-\pi^*$ transitions. It forms composites with AuNPs, affecting the visible light properties. The drop in Eg value that occurred with an increase in Au concentration may account for the creation of localized states (increase in the number of traps) between the highest occupied molecular orbital and the lowest empty molecular orbital energy bands. As a result, there would be more electronic transitions between the valence and the conduction bands [21].

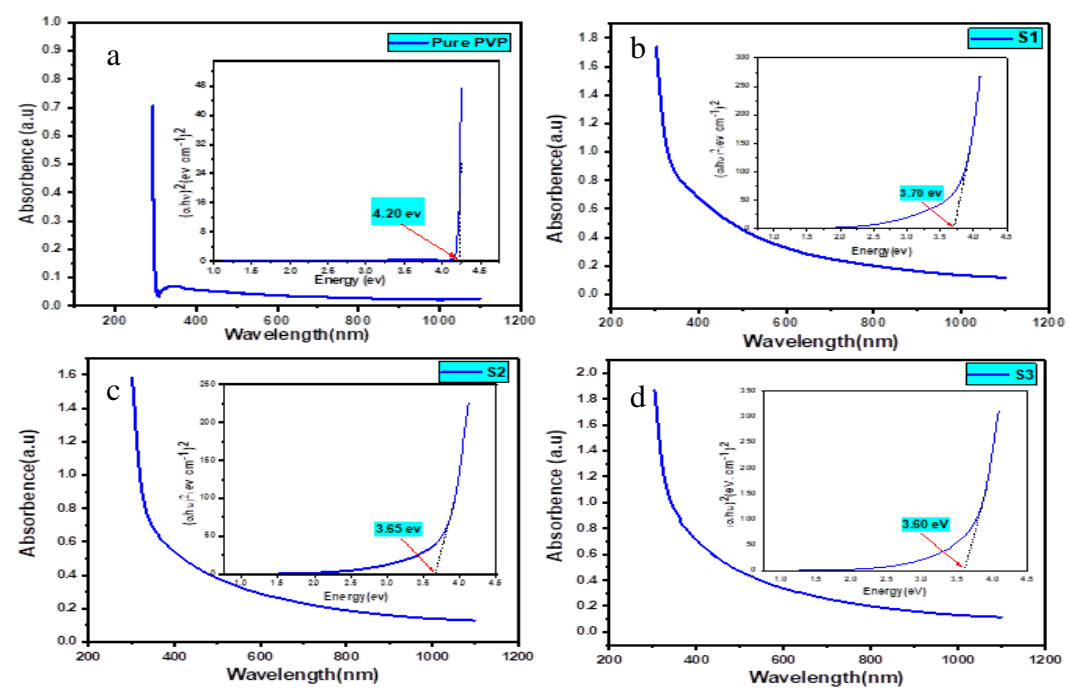


Figure 5: The absorbance spectrum and the magnitude of the energy gap for :(a)

Pure PVP, (b) S1, (c) S2, and (d) S3.

Sample	E _g (eV)		
Pure	4.20		
S 1	3.70		
S2	3.65		
S3	3.60		

Table 1: The direct energy bandgap values for all samples.

3. 4. The Fourier Transformation Infrared (FTIR)

The functional groups, determined by FTIR analysis as part of the characterization of the pure PVP nanofiber and the composite Au-PVP nanofiber with various mixing ratios, were produced by the electrospinning process using a DC voltage. The FTIR spectra of the nanofibers showed a prominent peak at wavenumber 3446 cm⁻¹ associated with the O-H bond, which stands for the hydroxyl group (Fig. 6). At the wavenumber 2952 cm⁻¹, the asymmetric stretching is related to the C-H bond. The PVP's distinctive peaks are observed at a wavenumber of 1655 cm⁻¹, which corresponds to the stretching of the C=O (carbonyl group). The C-H vibration is associated with the asymmetric stretching, showing a peak at 1514 cm⁻¹ for pure PVP nanofiber and at 1436 cm⁻¹ for the gold-doped version. At the 1288 cm⁻¹ wavelength, where the absorption peak occurred, there is a curvature toward the C-N vibration bond. The C-C bond bends at the absorption peaks 1014 and 833 cm⁻¹. These findings align with other studies [22, 23]. The FTIR measurements revealed that the addition of Au nanoparticles to PVP altered the location of the absorption peaks of the oscillations (Table 2). Some peaks appeared at a depth of 100 cm; these peaks indicate that the Au nanoparticles are present within the structure.

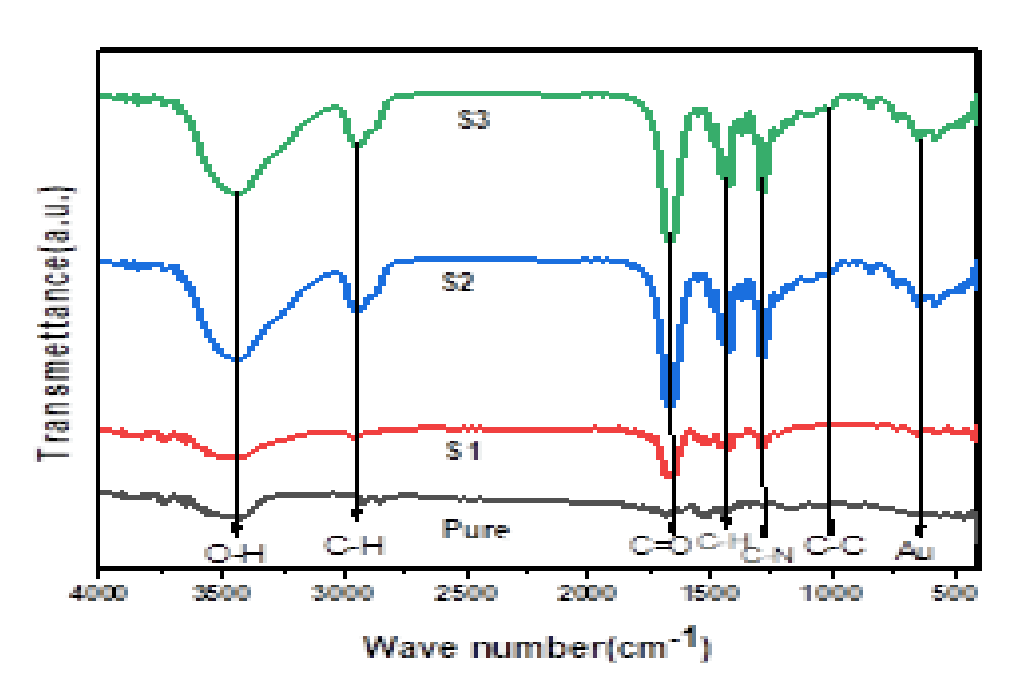


Figure 6: Infrared spectra of pure PVP and Au-PVP at different doping ratios.

Samples	O-H Stretch Vibration	C-H Stretch Vibration	C=O Stretch Vibration	C- H Stretch Vibration	C-N bending Vibration	C-C bending Vibration
Pure PVP	3446	2952	1661	1385	1308	1135
S1	3446	2952	1661	1411	1276	1006
S2	3446	2952	1661	1436	1276	1006
S3	3446	2952	1661	1436	1267	1006

Table 2: The absorption peaks of PVP mixed with Au at different doping ratios.

4. Detector Measurements

The most significant characteristics of photodetectors are their quick fall and response times. The Au-PVP films with different mixing ratios were coated on the n-Si substrate to improve the characteristics of the detector. The photosensitivity of the detector was assessed for each film. The time-dependent optical currents of the pure PVP organic polymer and of doped with different Au ratios (S1, S2, and S3) are shown in Fig. 7. The time-current properties (t-I) were determined with two different wavelengths of excitation 360 and 465 nm. The current of the detector was measured by exposing it to a light (light current); the lamp intensity was 40mw/cm^2 with light off (darkness current). According to the indicated optical features, a strong absorption is shown in that region, the findings revealed a great sensitivity and tracked the region near the UV region. It was found that there was a noticeable rise in the photocurrent with an increase in the doping ratios of gold nanoparticles. Sensitivity (S) is a measure of a sample's increase in current when exposed to light. Eq. (3) is used to determine the sensitivity values of PVP for pure and mixed with gold nanoparticles [24]:

$$S = \frac{I_{ph} - I_{d}}{I_{d}} \times 100\%$$
 (3)

where I_{ph} is light current and I_d is darkness current.

The conductivity increased when the light was turned on, and current returned to its starting point when the light off. It was clear that throughout this method, the rise and fall durations for each condition of the lights on and off are less than 20 sec. The results showed that the increase in the doping of Au nanoparticles with PVP has a significant increase in the surface area of the films, which in turns enhances the absorption ratio and the generation of charge carriers, boosting the sensitivity of the photodetector. This raises the possibility that the electron will be stimulated into the conduction band. An enhanced pulse shape of the photocurrent above the pure PVP pulse form suggests a quicker response to these light wavelengths. The analysis's findings demonstrated sample (S3) exhibited more photosensitivity than the other samples. As shown in Table 3, a good sensitivity was in the 465 nm source for the S1 sample (the sample with the lowest Au). The Au addition may enhance the sensitivity by the Surface Plasmon Resonance (SPR) effect, which causes an increase in photon absorption [25]. The sample (S3) with the highest Au showed the highest UV sensitivity of 24.45%.

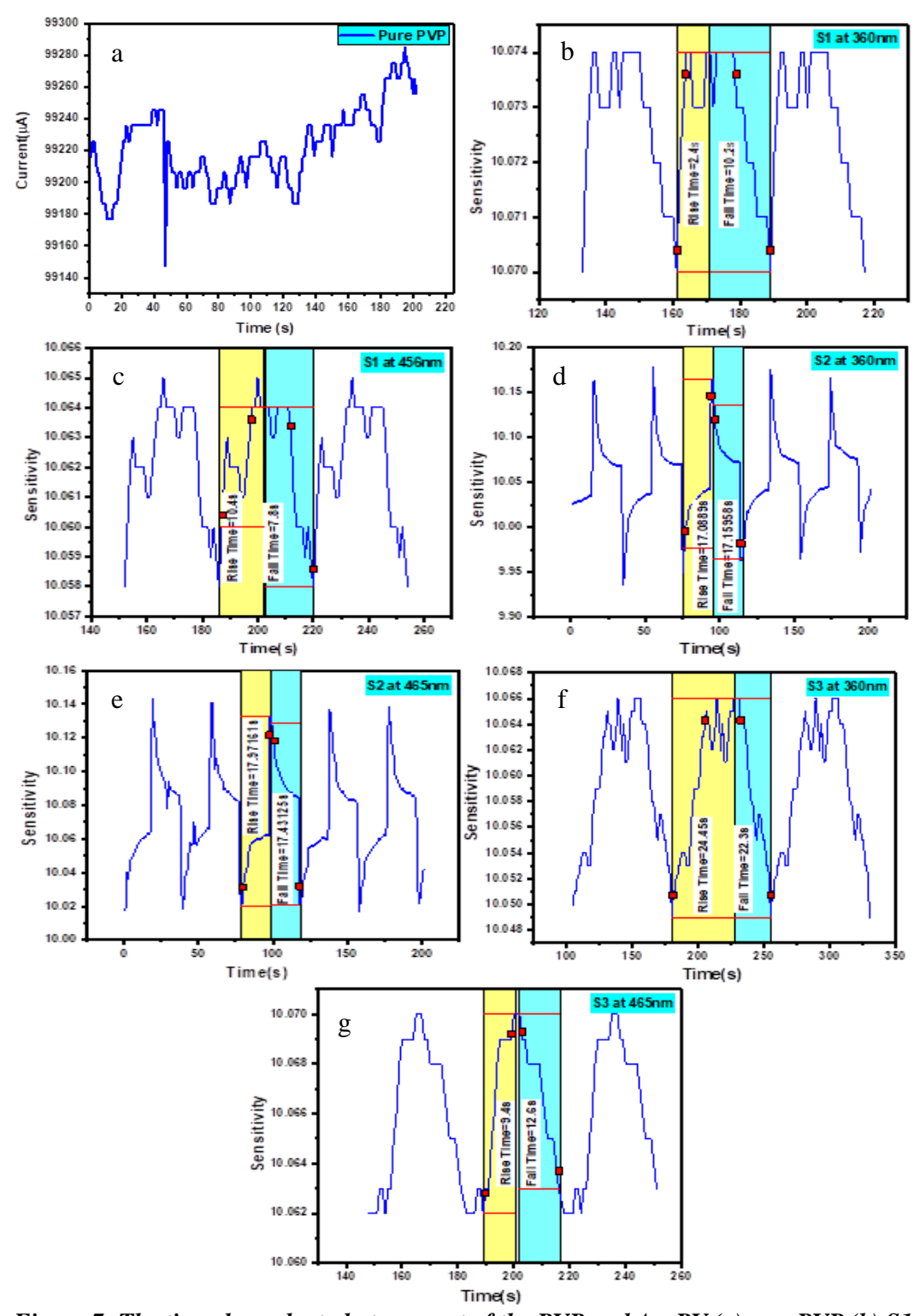


Figure 7: The time-dependent photocurrent of the PVP and Au-PV (a)pure PVP (b) S1 at360nm (c) S1 at465nm (d) S2 at360nm (e) S2 at465nm (f) S3 at360nm and (g) S3 at465nm.

Table 3: The sensitivity, response time and recovery time for PVP doped with different Au ratios at high voltage (20 kV).

Sample	S% at 360 nm	S % at 465 nm	t _{Res} (s) at 360 (nm)	t _{Res} (s) at 360 (nm)	t _{Res} (s) at 465 (nm)	t _{Res} (s) at 465 (nm)			
S1	2.4	10.4	2.4	10.2	10.4	7.8			
S2	17.0	17.9	17.0	18.0	17.9	17.4			
S3	24.45	9.40	24.45	22.30	9.40	12.60			

4. Conclusions

In this study, the PVP and Au-PVP nanofibers were successfully prepared by electrospinning. The XRD results showed an amorphous structure for all the samples. The FE-SEM images indicated the formation of nanofibers with attached beads and a decrease in the fibre diameter by adding Au. The Au-PVP nanocomposite showed a change in the optical energy gap from 4.20 to 3.60 eV and an enhanced absorption spectrum compared to the pure PVP nanofiber film. The UV detector improvement was achieved, and the high sensitivity of Au-PVP nanofiber for the produced sample S3 reached 24.45%. The variation in the sample characteristics and sensitivity with Au nanoparticlea addition have an effective result. The prepared samples are candidates for use in various healthcare and environmental monitoring applications.

Conflict of Interest

Authors declare that they have no conflict of interest.

References

- 1. S. Raza, X. Li, F. Soyekwo, D. Liao, Y. Xiang, and C. Liu, European Poly. J. **160**, 110773 (2021). https://doi.org/10.1016/j.eurpolymj.2021.110773.
- 2. K. M. Zaidan, H. F. Hussein, R. A. Talib, and A. K. Hassan, Ener. Proce. **6**, 85 (2011). https://doi.org/10.1016/j.egypro.2011.05.010.
- 3. S. Tajik, H. Beitollahi, F. G. Nejad, I. S. Shoaie, M. A. Khalilzadeh, M. S. Asl, Q. Van Le, K. Zhang, H. W. Jang, and M. J. R. A. Shokouhimehr, RSC Adv. 10, 37834 (2020). https://doi.org/10.1039/D0RA06160C.
- 4. P. Franco and I. De Marco, Polymers 12, 1114 (2020). https://doi.org/10.3390/polym12051114.
- 5. S. R. Mohammed, M. M. Ismail, and I. M. Ibrahim, J. Electrochem. En. Conv. Stor. **21**, 031002 (2023). https://doi.org/10.1115/1.4063303.
- 6. R. Ahmed, N. Hassan, and I. Ibrahim, Dig. J. Nanomat. Biostruct. **17**, 759 (2022). https://doi.org/10.15251/DJNB.2022.173.759.
- 7. H. J. Hassan, A. K. Abbas, and I. M. Ibrahim, AIP Conf. Proc. **2834**, 090006 (2023). https://doi.org/10.1063/5.0171846.
- 8. M. Teodorescu and M. Bercea, Poly. Plast. Tech. Eng. **54**, 923 (2015). https://doi.org/10.1080/03602559.2014.979506.
- 9. J. Xue, T. Wu, Y. Dai, and Y. Xia, Chem. Rev. **119**, 5298 (2019). https://doi.org/10.1021/acs.chemrev.8b00593.
- 10. B. Abadi, N. Goshtasbi, S. Bolourian, J. Tahsili, M. Adeli-Sardou, and H. Forootanfar, Front. Bioeng. Biotech. 10, 01 (2022). https://doi.org/10.3389/fbioe.2022.986975.
- 11. X. Chen, F. Ren, J. Ye, and S. Gu, Semiconductor Science and Technology, **35**, 023001 (2020). https://doi.org/10.1088/1361-6641/ab6102.
- 12. H. Wang, Y. Zhang, H. Niu, L. Wu, X. He, T. Xu, N. Wang, and Y. Yao, Comp. Part B Eng. **230**, 109505 (2022). https://doi.org/10.1016/j.compositesb.2021.109505.
- 13. A. Barhoum, K. Pal, H. Rahier, H. Uludag, I. S. Kim, and M. Bechelany, Appl. Mat. Today 17, 1 (2019). https://doi.org/10.1016/j.apmt.2019.06.015.
- 14. A. Newman, D. Engers, S. Bates, I. Ivanisevic, R. C. Kelly, and G. Zografi, J. Pharmaceut. Sci. **97**, 4840 (2008). https://doi.org/10.1002/jps.21352.
- 15. W. Gong, W. Yang, J. Zhou, S. Zhang, D.-G. Yu, and P. Liu, Nanocomposites **10**, 228 (2024). https://doi.org/10.1080/20550324.2024.2362477.
- 16. A. Ahmadian, A. Shafiee, N. Aliahmad, and M. Agarwal, Textiles 1, 206 (2021). https://doi.org/10.3390/textiles1020010.
- 17. D. Gupta, M. Jassal, and A. K. Agrawal, Poly. J. **51**, 883 (2019). https://doi.org/10.1038/s41428-019-0196-1.
- 18. Y. Liao, T. Fukuda, N. Kamata, and M. Tokunaga, Nanoscale Res. Lett. **9**, 267 (2014). https://doi.org/10.1186/1556-276X-9-267.
- 19. E. A. Davis and N. F. Mott, Philosoph. Mag.: A J. Theo. Exper. Appl. Phys. **22**, 0903 (1970). https://doi.org/10.1080/14786437008221061.
- 20. W. Matysiak, T. Tański, and M. Zaborowska, Bull. Pol. Ac.: Tech. **67**, 193 (2019). https://doi.org/10.24425/bpas.2019.128601.
- 21. O. G. Abdullah and S. A. Saleem, J. Electron. Mater. **45**, 5910 (2016). https://doi.org/10.1007/s11664-016-4797-6.

- 22. C. Virginia, A. Khasanah, J. Jauhari, and I. Sriyanti, IOP Conf. Ser.: Mater. Sci. Eng. **850**, 012039 (2020). https://doi.org/10.1088/1757-899X/850/1/012039.
- 23. D. Andjani, I. Sriyanti, A. Fauzi, D. Edikresnha, M. M. Munir, H. Rachmawati, and Khairurrijal, Proce. Eng. 170, 14 (2017). https://doi.org/10.1016/j.proeng.2017.03.003.
- 24. J.-M. Liu, Photonic Devices (Cambridge, Cambridge University Press, 2005). https://doi.org/10.1017/CBO9780511614255.
- 25. S.-W. Choi, H.-S. Kim, W.-S. Kang, J.-H. Kim, Y.-J. Cho, and J.-H. J. Kim, J. Nanosci. Nanotech. **8.** 4569 (2008). https://doi.org/10.1166/jnn.2008.IC58.

البرم الكهربائي لألياف PVP النانوية والمطعمة بجسيمات الذهب النانوية لكاشف البرم الكهربائي لألياف الاشعة الفوق البنفسجية

مروان سعيد عبدالحميد وعصام محمد ابراهيم القيرياء، كلية العلوم، جامعة بغداد، بغداد، العراق

الخلاصة

يهدف هذا العمل إلى تحضير ألياف نانوية من البولي فينيل بيروليدون (PVP) وألياف نانوية مركبة من Au-PVP بتركيزات مختلفة من الذهب باستخدام تقنية الغزل الكهربائي وتطبيق الجهد المستمر (20) كيلو فولت. على ركائز زجاجية ورقائق سيليكون من النوع (n-Si) باتجاه (111) عند درجة حرارة الغرفة. تمت دراسة تأثير المواد المضافة على بعض الخواص الفيزيائية (التركيبية، الضوئية، الكهربائية، والحساسية) لمادة البوليمر. تم فحص الخصائص الهيكلية والمورفولوجية والبصرية للمادة باستخدام XRD (XRD والأشعة فوق البنفسجية المرئية. كان هيكل Au-PVP غير متبلور كما يظهر من حيود الأشعة السينية. يتم تحضير ألياف الفيلم المركبة المصنوعة من الألياف النانوية Au-PVP مع ارتفاع تركيز Au-PVP. تراوحت فجوة الطاقة الضوئية لثلاثة ألياف نانوية Au-PVP مع ارتفاع تركيز Au-PVP كاشف الأشعة فوق البنفسجية، حيث كان الكاشف الأمثل عند الطول الموجي فولت، وتم الحصول على التوالي، وكانت قيم زمن الموحود تتراوح بين (24.45-28) و S3 على التوالي، وكانت قيم زمن الصعود تتراوح بين (24.45-24) ثانية) وزمن الهبوط (10.2-22.3 ثانية) لتركيزات الذهب.

الكلمات المفتاحية: PVP، ألياف النانو، الغزل الكهربائي، منشق مرن، فلم رقيق.